Ö.A. Erdogan et al. / Hacettepe J. Biol. & Chem., 2026, 54(1), 47-55

Research Article

Hacettepe Journal of Biology and Chemistry

journal homepage: https://hjbc.hacettepe.edu.tr/
Dergipark Akademik: https://dergipark.org.tr/en/pub/hjbc

Oleuropein Inhibits Cancer Stemness in a Dynamic 3D Breast Tumor Model

Dinamik 3B Meme Tümörü Modelinde Oleuropein Kanser Köklülüğünü Azaltmaktadır

Özlem Altundag Erdogan[1,2], Maryam Ghulam Sarwar[3], Betül Çelebi Saltik[1,2*]

[1]Department of Stem Cell Sciences, Hacettepe University Graduate School of Health Sciences, Ankara, Turkey.

[2]Center for Stem Cell Research and Development, Hacettepe University, Ankara, Turkey.

[3]Department of Botany, University of Peshawar, Peshawar, Pakistan.

ABSTRACT

Cancer stem cell transplantation (CSC) provides important insights into their role in promoting angiogenesis and metastasis through a variety of intense and stringent adaptations that depend on their interaction with the tumor microenvironment. We aimed to evaluate the biological responses of CSCs in a three-dimensional (3D) microenvironment after targeted treatment with oleuropein (OLE). TUNEL assays were recorded to assess apoptotic activity in spheroid structures. We demonstrated increased expression of *OCT3/4, NANOG, SOX2, SURVIVIN, CYCLIN-D1,* and *p21* in both static and dynamic cultures following OLE treatment by RT-qPCR. These findings collectively highlight the anti-proliferative and pro-apoptotic effects of OLE on CSCs.

Key Words
Breast cancer, MCF-7, stem cell, oleuropein.

ÖZ

Kanser kök hücrelerinin (KKH) tümör mikro çevresiyle etkileşiminin araştırılması,çeşitli hücresel ve moleküler adaptasyon mekanizmaları aracılığıyla anjiyogenez ve metastazı desteklemedeki rollerine dair önemli bilgiler sağlar. Bu çalışmada, oleuropein (OLE) ile hedefli tedaviden sonra KKH'lerin biyolojik yanıtlarını üç boyutlu (3B) bir mikro çevrede değerlendirmeyi amaçladık. Sferoid yapılarda apoptotik aktiviteyi değerlendirmek için TUNEL testi kullanıldı. OLE tedavisinin ardından, hem statik hem de dinamik kültürler *OCT3/4, NANOG, SOX2, SURVIVIN, CYCLIN-D1* ve *p21* ekspresyonunun arttığını RT-qPCR ile gösterdik. Bu bulgular topluca, OLE'nin kök hücreler üzerindeki anti-proliferatif ve pro-apoptotik etkilerini vurgulamaktadır.

Anahtar Kelimeler
Meme kanseri, MCF-7, kök hücre, oleuropein.

Article History: Jul 16, 2025; Accepted: Oct 14, 2025; Available Online: Dec 30, 2025.

DOI: https://doi.org/10.15671/hjbc.1743955

Correspondence to: B.Ç. Saltik, Department of Stem Cell Sciences, Hacettepe University Graduate School of Health Sciences, Ankara, Turkey.

E-Mail: betul.celebi@hacettepe.edu.tr

INTRODUCTION

Cancer stem cells (CSCs), as cells with self-renewal and multi-lineage differentiation potential similar to normal tissue stem cells, contribute to tumor heterogeneity [1]. These cells have self-renewal capacity and contribute to tumor initiation in multiple tumor malignancies, such as recurrence, metastasis, heterogeneity, multidrug resistance, and therapy resistance. CSCs constitute 0.1-1% of the entire heterogeneous tumor population and have been shown to be similar to normal stem cells with their ability for self-renewal, proliferation, and therapy resistance due to their quiescent state (cell cycle arrest) [2]. It is known that breast CSCs, known for their CD44+, CD24-/low profile, are also characterized by *in vitro* mammosphere formation/*in vivo* tumor formation [3]. The induction of cellular mechanisms that support CSCs to be resistant to chemotherapy/radiotherapy and their quiescent state necessitates the determination of new treatment strategies. Widely used chemotherapy agents target proliferating cells to direct them to apoptosis. Therefore, although it is known that most of the proliferating tumor cells are eliminated in successful cancer treatments, CSCs with higher invasiveness and resistant survival abilities can induce cancer recurrence [4, 5].

In recent years, personalized approaches to cancer treatment have garnered significant interest. In this context, studies on testing various anti-cancer agent combinations of patient-derived tumor cells in a three-dimensional (3D) environment and mimicking the tumor environment have gained momentum in recent years [6]. Djomehri et al. created a breast cancer organoid model by co-culturing MCF-10A epithelial cells with MDA-MB-231 cells to mimic tissue-like structure by using ultra-low attachment plates and matrigel [7]. It has been reported that MCF-7 cells in different 3D-hydrogel conditions such as matrigel, alginate and hyaluronic acid overexpress pro-angiogenic growth factors, have increased tumorigenic properties, are insensitive to drug therapy, and have high malignancy in *in vivo* experiments [8-12].

Various studies have demonstrated that the anti-angiogenic secoiridoid Oleuropein (OLE) obtained from olive tree (especially leaves), irreversibly and dose-dependently inhibits the proliferation, invasion and replication of cancer cells, unlike normal cells [13]. Han et al. showed that HT and OLE, decreased cell viability and proliferation of MCF-7 by arresting cells in G1/S phase, triggered cell apoptosis [14]. Lu et al. found that MDA-MB-231 cells were treated with HT and OLE in combination with Hepatocyte Growth Factor (HGF), rapamycin, or 3-methyladenine (3-MA), and analyzed for cell viability, migration, invasion, and autophagy signaling. As a result, treatment with HT/OLE reduced cell viability dose-dependently, and both HT and OLE was found to inhibit the migration and invasion induced by HGF or 3-MA by activating autophagy [15]. In another study, after exposing MDA-MB-231 (100–700 μM) and MDA-MB-468 (100-400 μM) TNBCs to commercially acquired OLE for 48 hours (h), 72 h and 96 h, OLE to both cell groups resulted in cytotoxic effects. This was confirmed by the decrease in IC50 values from 159.70 to 92.43 μM in MDA-MB-468 cells and from 225.65 to 98.78 μM in MDA-MB-231 cells between the 72h and 96h time periods [16]. In addition, Elamin et. al discovered that OLE treatment results in a significant decrease in cell viability of MCF-7 and MDA-MB-231 cells by triggering mitochondrial pathway-mediated apoptosis, leading to S-phase arrest in the cell cycle. Moreover, the apoptotic effect of OLE was detected selectively in cancer cells without affecting non-tumorigenic MCF-10A epithelial cells [17]. Asgharzade et al. showed that OLE induces apoptosis in MCF-7 and MDA-MB-231 cells by causing onco-miR and anti-apoptotic gene down-regulation, up-regulation of tumor suppressor miRNA and pro-apoptotic genes [18]. Tezcan et al. found that the combination of olive leaf extract and bevacizumab resulted in a significant reduction in tumor size, vascularization, and migration of glioblastoma cells [19]. Although there are various studies on the effects of OLE in various tumor types and CSCs, this mechanism has not been fully elucidated and detailed with the concept of breast CSCs. Fluidic chip systems are an approach that can manipulate fluids on a microscopic scale, thereby controlling cell culture-related parameters to better stimulate the microenvironment of tumor tissues *in vivo* [20]. Recently, Chakrabarty et al. designed microfluidic cancer on a chip platform that maintained cell viability, proliferation, and tissue morphology for at least 14 days for breast cancer PDX slices [21]. Zhai et al. validated a microfluidic system for single and multi-drug screening involved testing of the drug toxicity of two chemotherapeutics, cisplatin (Cis) and epirubicin (EP), on MDA-MB-231 and MCF-10A cell lines. They reported that their results were consistent with those screened based on traditional 96-well plates.

These findings demonstrated the reliability of the drug screening system with an on-chip system [22].

In our prior research conducted by our group, treatment of 200 µg/mL OLE-loaded mALG microparticles inhibited the epithelial-to-mesenchymal transition by reducing the expression of Vimentin and Slug proteins, while simultaneously elevating the levels of E-cadherin in the 3D breast cancer model we developed using CSCs, MCF-12A, and HUVECs [23]. In this study, our primary objective is to selectively target therapeutically resistant CSCs utilizing OLE within the complex 3D architecture of a heterogeneous tumor microenvironment. Our experimental design involved the creation of a 3D breast cancer model incorporating CSCs and non-tumorigenic MCF-12A cells, embedded within a supportive matrix of Methocel/Matrigel/Collagen-I, and subsequently vascularized with HUVECs. Then, the heterogeneous tumor population was treated with 200 µg/mL OLE both in static and microfluidic (dynamic) culture systems. Subsequently, CSC apoptosis (TUNEL assay), stemness (*OCT3/4, NANOG, SOX2*), ABC transporters (*ABCG1, ABCG2),* metastatic properties (*CXCR4)* and proliferation (*SURVIVIN, p21, CYCLIN D1*) related gene expressions were evaluated by RT-qPCR.

MATERIALS and METHODS

Cell Culture

MCF-7 human breast cancer cell line (ATCC) was grown in RPMI 1640 (Gibco) supplemented with 10% FBS (Capricorn), L-glutamine (Sigma) and penicillin/streptomycin (Sigma) in a humidified incubator at 37°C with 5% CO2. The non-tumorigenic epithelial cell line MCF-12A (ATCC) was cultured in DMEM/F12 (Capricorn) supplemented with Nu serum (corning), ITS premix (Corning), penicillin/streptomycin, L-glutamine. HUVECs were cultured in EGM-2 (Lonza) medium supplemented with FBS, penicillin/streptomycin and L-glutamine. The cell culture was maintained by replacing the medium every three days until reaching 70-80 % confluency.

This study did not involve any human participants or human tissue, nor did it include the use of live animals or vertebrate models. Therefore, ethical approval by an institutional review board or ethics committee was not required, in accordance with relevant national and institutional guidelines.

Isolation and characterization of cancer stem cells

MCF-7 CSCs were isolated from 70-80% confluent MCF-7 cells using the Magnetic-Activated Cell Sorting (MACS) technique with CD44 and CD24 magnetic beads (Miltenyi Biotech), following the manufacturer's protocol (n=3). For CSC characterization using FACS analysis, the isolated cell pellet was resuspended in FACS buffer and labeled with anti-CD24-PE (Biolegend) and anti-CD44-FITC (Biolegend) antibodies. Following a 30-minute incubation at room temperature, cell surface markers CD44 and CD24 were assessed using the BD Accuri TM C6 Flow Cytometer (BD Bioscience). mRNA quantification of *OCT3/4, NANOG, SOX2, ABCG1*, and *ABCG2* was carried out via RT-qPCR to elucidate differences gene expression between MCF-7 cells and isolated CSCs. The expression levels of selected genes and reference gene (GAPDH) were measured comparatively using the Light Cycler® 480 II (Roche, Germany) Total cellular RNA was isolated using the general RNA isolation kit (Hibrigen). The isolated RNA concentration was measured at 260 nm using the NanoDrop ND-1000 spectrophotometer (ThermoFisher Scientific Inc., USA) and the A260/A280 ratio was used to measure the RNA extraction quality. Complementary deoxyribonucleic acid (cDNA) synthesis was performed from RNA samples using iScript cDNA synthesis kit (Bio-Rad). Quantitative PCR condition: 10 min denaturation step at 95°C; A total of 45 cycles was set as a PCR step at 95°C for 10 seconds, at 60°C for 30 seconds, at 72°C for 1 second, and at 40°C for 30 seconds as a cooling step. Three biological replicates were run for each different experimental condition, and three technical replicates were performed for each sample. Crossing point (Cp) or threshold cycle (Ct) value was calculated for target and reference genes using LightCycler® 480 II software (n=3).

Design of the dynamic condition

The microfluidic device was obtained with polydimethylsiloxane (PDMS, Fisher), an elastomeric material. The layer of the microfluidic chip was prepared by cutting polymethyl methacrylate blocks with a laser cutter, using them as molds and pouring PDMS. The gas inside was cured in an oven at 65°C for > 4h. The devices were activated by air plasma. The chamber diameter was designed as 18 mm. The fluid flow was provided by the pump (VWR) at 10mL/min.

Generation of the 3D breast cancer model inside of the dynamic system

Co-culture of CSCs isolated with MCF-12A epithelial cells was performed by mixing the cells and cell media in a 1:1 ratio.CSC culture medium was prepared with RPMI 1640 (no phenol red, Gibco) supplemented by EGF (Sigma), B-27 (Sigma), L-glutamine (Sigma) and penicillin/streptomycin (Sigma). To support the organoid structure, methylcellulose (Methocel® MC, Fluka), matrigel (Sigma) and Collagen-I was added to the cell suspension and culture was maintained for three days by changing the medium. HUVECs were then added to vascularize the 3D structure and cultured for an additional four days. Half of the culture medium was removed, and culture was continued with the addition of fresh medium. The treatment of 3D co-culture cells with 200 µg/mL. Subsequent analyses were performed following OLE treatment in both static and dynamic culture environments.

TUNEL assay

The TUNEL Assay Kit HRP-DAB (Abcam) was executed following the manufacturer's instructions. On the seventh day of culture, the 3D cancer model was exposed to 200 µg/mL OLE for 7h. A separate 3D cancer model without OLE treatment served as the control group. Following PBS washes, all experimental conditions (both control and OLE-treated groups) were fixed with 4% paraformaldehyde for thirty minutes. Subsequently, the protocol provided by the kit was followed, and apoptotic cells were observed using a microscope (OLYMPUS CKX41).

Gene expression analysis

RT-qPCR analysis was performed to evaluate gene expressions in OLE-targeted cells in static and dynamic cultures. Expression levels of genes (*NANOG, OCT3/4, SOX2, SURVIVIN, CYCLIN D1, p21, ABCG1, ABCG2, CXCR4*) and reference gene *GAPDH* were measured comparatively using the LightCycler® 480 II (Roche, Germany) Total cellular RNA was isolated using the general RNA isolation kit (Hibrigen). The isolated RNA concentration was measured at 260 nm using the NanoDrop ND-1000 spectrophotometer (Thermo Fisher Scientific Inc., USA) and the A260/A280 ratio was used to measure the RNA extraction quality. Complementary deoxyribonucleic acid (cDNA) synthesis was performed from RNA samples using iScript cDNA synthesis kit (Bio-Rad). The quantitative PCR conditions were as follows: 10 min denaturation step at 95°C; A total of 45 cycles was set as a PCR step at 95°C for 10 seconds, at 60°C for 30 seconds, at 72°C for 1 second, and at 40°C for 30 seconds as a cooling step. Three biological replicates were run for each different experimental condition, and three technical replicates were performed for each sample. Crossing point (Cp) or threshold cycle (Ct) value was calculated for target and reference genes using LightCycler® 480 II software (n=3).

Statistical analysis

Statistical analyzes SPSS Inc. Comparisons between different experimental groups were made with the help of t-test, and ANOVA. Data with a p-value less than 0.05 were considered statistically significant. Unless otherwise stated, each sample was run three times.

RESULTS and DISCUSSION

Characterization of MCF-7 and CD44+/CD24- cancer stem cells (CSCs)

Experiments were initiated when MCF-7 cells showed adherence to the culture dish and reached 70-80% confluency. Then, MACS-sorted CSCs from MCF-7 were morphologically characterized by colony formation as semi-suspended spheres over five days (Figure 1a).

Although conventional 2D cell culture systems offer a suitable environment for studying cancer cells, they are insufficient to mimic tumor structures because they do not include microenvironmental parameters such as cell-cell communications and extracellular matrix (ECM) interactions that play critical roles in cancer cells. Cells cultured in 2D adapt to sheet-like morphology and are forced to alter their cell growth, migration, and apoptosis responses. Therefore, cell-cell interactions, epithelial to mesenchymal transition (EMT) and the effects of drugs acting on CSCs are also reduced. 3D systems offer an important alternative way to overcome this problem [24]. MDA-MB-231 embedded spheroid tumor model exhibited the most robust response to chemotherapeutic treatment and possessed the greatest CSC content [25]. In this study, we examined the effect of anti-tumorigenic OLE on CSCs by creating an ECM support composed of 3D collagen, methylcellulose and matrigel and cellular microenvironment with MCF-12A and HUVEC, mimicking the *in vivo* structure. Before targeting the 3D breast cancer model, we examined the morphological (Figure 1a) and molecular (Figure 1b) differences between the MCF-7 cell line and CD44+/24- breast CSCs.

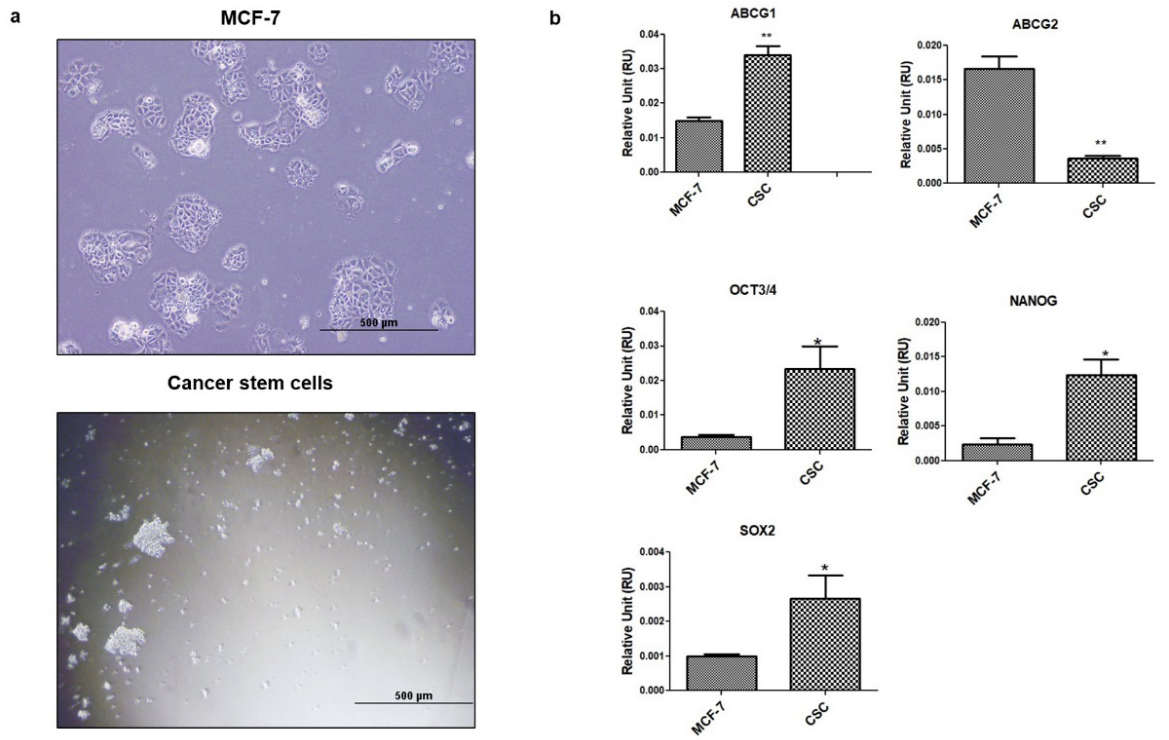

Figure 1. Characterization of MCF-7 and CD44+/CD24- cancer stem cells (CSCs). a) Morphology of MCF-7 and CD44+/CD24- CSCs in culture. Scale bar: 500 µm. b) Evaluation of gene expressions of MCF-7 and CD44+/CD24- CSCs in culture by RT-qPCR. CSC: cancer stem cell. *: p<0.05, **: p<0.01, n=3. OCT3/4: Octamer-Binding Transcription Factor 3/4, NANOG: Homeobox protein, SOX2: SRY-Box Transcription Factor 2, ABCG1: ATP Binding Cassette Subfamily G Member 1, ABCG2: ATP Binding Cassette Subfamily G Member 2.

RT-qPCR results *of ABCG1, ABCG2, OCT3/4, NANOG* and *SOX2* gene expressions of CSCs and MCF-7 cells are presented (Figure 1b). *ABCG1, OCT3/4, NANOG* and *SOX2* mRNA gene expressions were approximately 2.3-fold (p<0.01), 6.4-fold (p<0.05), 5.3-fold (p<0.05) and 2.7-fold (p<0.05) higher in CSCs compared to MCF-7 cells, respectively (n=3). On the other hand, *ABCG2* gene expression was approximately higher in MCF-7 cells compared to CSCs (4-fold, p<0.01). While MCF-7 had adherent cell morphology in the culture plate, CSCs formed embryonic stem cell (ESC)-like colonies in suspension. In addition, we detected higher *OCT3/4*, *NANOG* and *SOX-2* expressions in CSCs compared to MCF-7 cells (Figure 1b). It has been known that *OCT3/4, SOX2* and *NANOG* are core pluripotency master regulators in maintaining the pluripotent state and self-renewal in stem cells, as well as contributing to tumorigenesis and providing stem cell-like properties to cancer cells [26, 27]. Similarly, Linget al. reported high expression of pluripotency genes in both MCF7 and MDA-MB-231 cells to define stem-like cell profile [28]. Although the roles of ATP-binding cassette (ABC) transporters have not been fully studied and clarified, *ABCG1* has an essential role in tumor development in metastatic cancers and that knock down of *ABCG1* cause a decrease in the size of tumor by the accumulation of extracellular vesicles [29]. Similarly, *ABCG2* is reported to be an essential marker of tumor-initiating CSCs in therapy-resistant tumors [30]. Although we found A*BCG1* expression level higher (2.3-fold, p<0.01) in CSCs than MCF-7 cells, we observed the opposite for *ABCG2* (4-fold, p<0.01) expression. Based on this result, it can be interpreted that the heterogeneous tumor population may trigger expression of the *ABCG2* gene, which is associated with drug resistance compared to CD44+/CD24- cells alone.

Targeting 3D breast cancer model with OLE in static and dynamic conditions

The microfluidic layer consisting of PDMS and designed with a chamber diameter of 18 mm, in which polymethyl methacrylate blocks are cut with a laser cutter and used as a mold. The fluid flow was provided by the pump (VWR) and the system was prepared to target 3D cancer model with OLE for 7h (Figure 2).

Evaluation of apoptosis and cancer-related gene expression profile after OLE treatment

It has been shown in Figure 3a that the cells in 3D model before OLE treatment were stained blue (static=control group) and apoptotic cells after OLE treatment were stained brown (dynamic group). Stemness genes (*OCT3/4, NANOG and SOX2)* were increased in both static and dynamic culture after 200 µg/mL for 7h OLE treatment compared to control (Figure 3b).

OLE treatment in dynamic condition reduced the expression of *OCT3/4* (10-fold), *NANOG* (40-fold), and *SOX2* (2-fold) genes relative to static culture ($p<0.001$, n=3). Similarly, expression of apoptosis and cell cycle-related genes (*p21* and *CYCLIN D1*) was also increased following OLE treatment in static and dynamic conditions compared to control. OLE treatment in the dynamic system reduced the expressions of *SURVIVIN* (6.7-fold, $p<0.001$), *p21* (5.0-fold, $p<0.001$) and *CYCLIN D1* (1.7-fold, $p>0.05$) compared to OLE treatment in static culture (n=3). *ABCG1* ($p<0.001$) and *ABCG2* ($p<0.01$) gene expressions were detected in the control group, but not in the OLE-treated groups in static and dynamic culture (n=3). In addition, although CXCR4 gene expression tended to increase among OLE treatment groups in control, static and dynamic culture, respectively, it was not statistically significant. We targeted CSCs within 3D breast cancer model with 200 µg/mL OLE in both fluidic and static culture (Figure 2) for 7h. It was determined by TUNEL assay that OLE, whose cytotoxicity was reported in cancer cells, caused an increase in brown-stained apoptotic cells (Figure 3a). As a result of RT-qPCR analysis, it was found that the expressions of stemness genes *OCT3/4, NANOG, SOX2* were higher in cells in static culture compared to those in dynamic culture (Figure 3b). In a study examining the effect of HT on the transcriptional activity of HIF-2α, it was reported that HT did not affect the transcription of *OCT3/4* in breast cancer tissue cells [31]. On the contrary, they reported that secoiridoid decarboxymethyl oleuropein aglycone inhibited mammosphere formation in breast CSCs, caused a decrease in CD44+/CD24- and ALDH positive cell profile, and stemness gene *OCT4* expression showed a significant decrease in cancer cells after treatment [32]. Similarly, our findings indicated that *OCT4* expression is more suppressed in CSCs targeted with the fluidic system compared to static cultured cells. In addition, another study shows that *SOX2* has an important role in breast cancer stem cells and early breast cancer development, representing an early step in breast tumor initiation [33]. OLE has been reported to exhibit specific cytotoxicity against MDA-MB-231 and MCF-7 breast cancer cells [17]. It has been demonstrated that OLE delays the cell cycle in the S phase, leading to inhibition of cell proliferation and up-regulation of the cyclin-dependent inhibitor

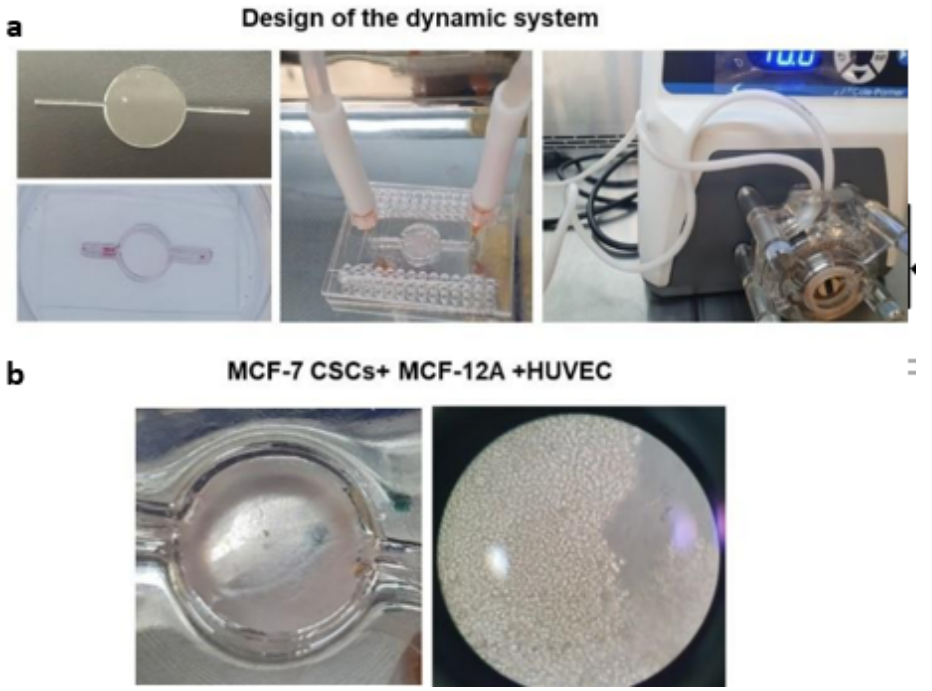

Figure 2. Three-dimensional (3D) dynamic system and targeting breast cancer model with OLE. a) Design of microfluidic system components b) Targeting of three-dimensional cancer cultured in the system with media containing OLE at 10 min/ml fluid circulation.

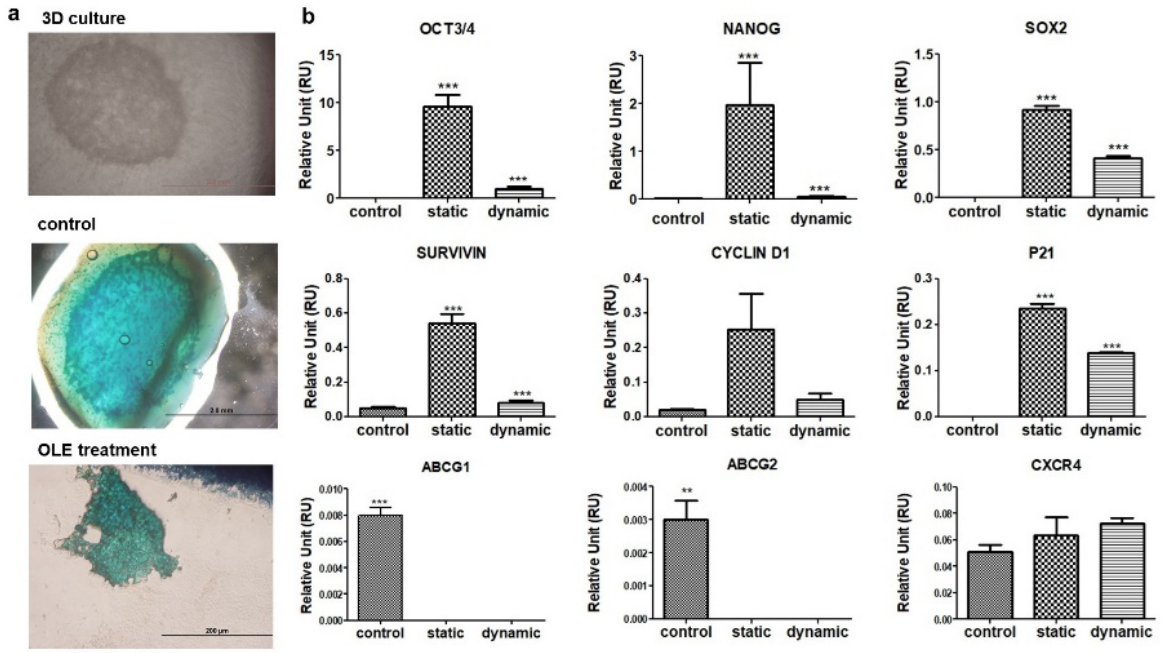

Figure 3. Results of 200 µg/mL OLE treatment (7h) on 3D breast cancer model. a) Effect of OLE on 3D cancer model. Scale bar: 2.0 mm, 200 µm. b) Effect of OLE on stemness, resistance, apoptosis and tumorigenicity related gene expressions.

*: p<0.05, **: p<0.01, ***: p<0.001, n=3. Control: Non-treated with OLE (0 µM), static: OLE treatment in static culture, dynamic: OLE treatment via fluidic system. *OCT3/4*: Octamer-Binding Transcription Factor 3/4, *NANOG*: Homeobox protein, *SOX2*: SRY-Box Transcription Factor 2, *ABCG1*: ATP Binding Cassette Subfamily G Member 1, ABCG2: ATP Binding Cassette Subfamily G Member 2, *CYCLIN D1*: CCND1, *p21*: CDKN1A, *SURVIVIN*: BIRC5, *CXCR4*: C-X-C Motif Chemokine Receptor 4.

p21. In the same study, it was determined that OLE inhibited anti-apoptosis and cell proliferation, which are specific mechanisms for cancer cells, and this was achieved by cyclin D1 inhibition. Erdogan et al. reported that apigenin flavonoid in olive oil dose-dependently inhibited cell survival by upregulation of *p21* and *p27* in prostate CSCs and decreased the migration of CD44+ CSCs [34]. Similarly, we found a decrease in cyclin D1 mRNA level and an increase in p21 level in CSCs targeted with OLE in dynamic condition. Although we detected *ABCG1* and *ABCG2* gene expressions in control group, which are associated with chemoresistance, tumor progression and stem-like profile in many cancers [29, 30, 35], we did not detect them in cells targeted with OLE in static and dynamic culture (Figure 3b). Thus, OLE exerts an apoptotic effect through a mechanism that suppresses the expression of genes that cause therapy resistance in these cells. All these findings highlight the necessity of investigating the benefit of oleuropein in breast cancer, especially in preventing/treating cancer stem cells that are less responsive to treatment.

CONCLUSION

The development of specific treatment for therapy-resistant cancer stem cells is important to prevent tumor recurrence and metastasis after treatment. Various approaches must be developed for effective drug development and appropriate delivery. In this study, we targeted the model that we created by mimicking the 3D microenvironment with OLE, which is known to have apoptotic effect in cancer cells, unlike normal tissue cells. We compared cell cycle, stemness, therapy resistance, and metastasis-related gene expressions in static and dynamic culture after OLE treatment. We demonstrated that tumorigenic properties were suppressed more effectively in dynamic culture in TNBC MDA-MB-231 CSCs. For further studies, the 3D model can be detailed and studied with immune cells and various microenvironmental components that contribute to cancer in the microenvironment. In the future, this study could be expanded to evaluate the efficacy of targeted various drugs on CSCs within the 3D spheroid structure created with a fluidic system. Besides, the model could be developed within a 3D structure that includes immune cells and various stromal cells. The response of the microenvironment to the drug can be evaluated by conducting drug trials on different tumor cells and on cancerous/non-cancer populations.

Acknowledgments
This work was supported by Hacettepe University Scientific Research and Projects Unit, Project No: TSA-2019-18405.

References

1. L. Yang, P. Shi, G. Zhao, J. Xu, W. Peng, J. Zhang, G. Zhang, X. Wang, Z. Dong, F. Chen, H. Cui, Targeting cancer stem cell pathways for cancer therapy, Signal Transduct. Target Ther., 5(1) (2020) 8.
2. R.X. Huang, E.K. Rofstad, Cancer stem cells (CSCs), cervical CSCs and targeted therapies, Oncotarget, 8(21) (2017) 35351-35367.
3. J. Stingl, Detection and analysis of mammary gland stem cells, J Pathol., 217(2) (2009) 229-241.
4. D.R. Pattabiraman, R.A. Weinberg, Tackling the cancer stem cells - what challenges do they pose?, Nat. Rev. Drug Discov., 13(7) (2014) 497-512.
5. Z.J. Yang, R.J. Wechsler-Reya, Hit 'em where they live: targeting the cancer stem cell niche, Cancer Cell, 11(1) (2007) 3-5.
6. J. Yu, W. Huang, The Progress and Clinical Application of Breast Cancer Organoids, Int. J. Stem Cells, 13(3) (2020) 295-304.
7. S.I. Djomehri, B. Burman, M.E. Gonzalez, S. Takayama, C.G. Kleer, A reproducible scaffold-free 3D organoid model to study neoplastic progression in breast cancer, J. Cell Commun. Signal., 13(1) (2019) 129-143.
8. C. Fischbach, R. Chen, T. Matsumoto, T. Schmelzle, J.S. Brugge, P.J. Polverini, D.J. Mooney, Engineering tumors with 3D scaffolds, Nat. Methods, 4(10) (2007) 855-60.
9. V. Harma, J. Virtanen, R. Makela, A. Happonen, J.P. Mpindi, M. Knuuttila, P. Kohonen, J. Lotjonen, O. Kallioniemi, M. Nees, A comprehensive panel of three-dimensional models for studies of prostate cancer growth, invasion and drug responses, PLoS One, 5(5) (2010) e10431.
10. R. Poincloux, O. Collin, F. Lizarraga, M. Romao, M. Debray, M. Piel, P. Chavrier, Contractility of the cell rear drives invasion of breast tumor cells in 3D Matrigel, Proc. Natl. Acad. Sci. U.S.A., 108(5) (2011) 1943-8.
11. C. Fischbach, H.J. Kong, S.X. Hsiong, M.B. Evangelista, W. Yuen, D.J. Mooney, Cancer cell angiogenic capability is regulated by 3D culture and integrin engagement, P. Natl. Acad. Sci. U.S.A., 106(2) (2009) 399-404.
12. L.A. Gurski, A.K. Jha, C. Zhang, X.Q. Jia, M.C. Farach-Carson, Hyaluronic acid-based hydrogels as 3D matrices for *in vitro* evaluation of chemotherapeutic drugs using poorly adherent prostate cancer cells, Biomaterials, 30(30) (2009) 6076-6085.
13. H.K. Hamdi, R. Castellon, Oleuropein, a non-toxic olive iridoid, is an anti-tumor agent and cytoskeleton disruptor, Biochem. Biophys. Res. Commun., 334(3) (2005) 769-78.
14. J. Han, T.P. Talorete, P. Yamada, H. Isoda, Anti-proliferative and apoptotic effects of oleuropein and hydroxytyrosol on human breast cancer MCF-7 cells, Cytotechnology, 59(1) (2009) 45-53.
15. H.Y. Lu, J.S. Zhu, Z. Zhang, W.J. Shen, S. Jiang, Y.F. Long, B. Wu, T. Ding, F. Huan, S.L. Wang, Hydroxytyrosol and Oleuropein Inhibit Migration and Invasion of MDA-MB-231 Triple-Negative Breast Cancer Cell via Induction of Autophagy, Anti-cancer Agents Med. Chem., 19(16) (2019) 1983-1990.
16. S.S. Messeha, N.O. Zarmouh, A. Asiri, K.F.A. Soliman, Gene Expression Alterations Associated with Oleuropein-Induced Antiproliferative Effects and S-Phase Cell Cycle Arrest in Triple-Negative Breast Cancer Cells, Nutrients, 12(12) (2020) 3755.
17. M.H. Elamin, M.H. Daghestani, S.A. Omer, M.A. Elobeid, P. Virk, E.M. Al-Olayan, Z.K. Hassan, O.B. Mohammed, A. Aboussekhra, Olive oil oleuropein has anti-breast cancer properties with higher efficiency on ER-negative cells, Food Chem. Toxicol., 53 (2013) 310-6.
18. S. Asgharzade, S.H. Sheikhshabani, E. Ghasempour, R. Heidari, S. Rahmati, M. Mohammadi, A. Jazaeri, Z. Amini-Farsani, The effect of oleuropein on apoptotic pathway regulators in breast cancer cells, Eur. J. Pharmacol., 886 (2020) 173509.
19. G. Tezcan, M.O. Taskapilioglu, B. Tunca, A. Bekar, H. Demirci, H. Kocaeli, S.A. Aksoy, U. Egeli, G. Cecener, S. Tolunay, Olea europaea leaf extract and bevacizumab synergistically exhibit beneficial efficacy upon human glioblastoma cancer stem cells through reducing angiogenesis and invasion *in vitro*, Biomed. Pharmacother., 90 (2017) 713-723.
20. Q.R. Guo, L.L. Zhang, J.F. Liu, Z. Li, J.J. Li, W.M. Zhou, H. Wang, J.Q. Li, D.Y. Liu, X.Y. Yu, J.Y. Zhang, Multifunctional microfluidic chip for cancer diagnosis and treatment, Nanotheranostics, 5(1) (2021) 73-89.
21. S. Chakrabarty, W.F. Quiros-Solano, M.M.P. Kuijten, B. Haspels, S. Mallya, C.S.Y. Lo, A. Othman, C. Silvestri, A. van de Stolpe, N. Gaio, H. Odijk, M. van de Ven, C.M.A. de Ridder, W.M. van Weerden, J. Jonkers, R. Dekker, N. Taneja, R. Kanaar, D.C. van Gent, A Microfluidic Cancer-on-Chip Platform Predicts Drug Response Using Organotypic Tumor Slice Culture, Cancer Res., 82(3) (2022) 510-520.
22. J. Zhai, C. Li, H. Li, S. Yi, N. Yang, K. Miao, C. Deng, Y. Jia, P.I. Mak, R.P. Martins, Cancer drug screening with an on-chip multi-drug dispenser in digital microfluidics, Lab Chip, 21(24) (2021) 4749-4759.
23. O. Altundag-Erdogan, R. Tutar, E. Yuce, B. Celebi-Saltik, Targeting resistant breast cancer stem cells in a three-dimensional culture model with oleuropein encapsulated in methacrylated alginate microparticles, Daru J. Pharm. Sci., (2024) 2(2) 471-483.
24. A.R. Aref, R.Y. Huang, W. Yu, K.N. Chua, W. Sun, T.Y. Tu, J. Bai, W.J. Sim, I.K. Zervantonakis, J.P. Thiery, R.D. Kamm, Screening therapeutic EMT blocking agents in a three-dimensional microenvironment, Integr. Biol. (Camb.), 5(2) (2013) 381-9.
25. D.S. Reynolds, K.M. Tevis, W.A. Blessing, Y.L. Colson, M.H. Zaman, M.W. Grinstaff, Breast Cancer Spheroids Reveal a Differential Cancer Stem Cell Response to Chemotherapeutic Treatment, Sci. Rep., 7(1) (2017) 10382.
26. M.M. Matin, J.R. Walsh, P.J. Gokhale, J.S. Draper, A.R. Bahrami, I. Morton, H.D. Moore, P.W. Andrews, Specific knockdown of Oct4 and beta2-microglobulin expression by RNA interference in human embryonic stem cells and embryonic carcinoma cells, Stem Cells, 22(5) (2004) 659-68.
27. A.C. Hepburn, R.E. Steele, R. Veeratterapillay, L. Wilson, E.E. Kounatidou, A. Barnard, P. Berry, J.R. Cassidy, M. Moad, A. El-Sherif, L. Gaughan, I.G. Mills, C.N. Robson, R. Heer, The induction of core pluripotency master regulators in cancers defines poor clinical outcomes and treatment resistance, Oncogene, 38(22) (2019) 4412-4424.

28. G.Q. Ling, D.B. Chen, B.Q. Wang, L.S. Zhang, Expression of the pluripotency markers Oct3/4, Nanog and Sox2 in human breast cancer cell lines, Oncol. Lett., 4(6) (2012) 1264-1268.
29. Y. Namba, C. Sogawa, Y. Okusha, H. Kawai, M. Itagaki, K. Ono, J. Murakami, E. Aoyama, K. Ohyama, J.I. Asaumi, M. Takigawa, K. Okamoto, S.K. Calderwood, K.I. Kozaki, T. Eguchi, Depletion of Lipid Efflux Pump ABCG1 Triggers the Intracellular Accumulation of Extracellular Vesicles and Reduces Aggregation and Tumorigenesis of Metastatic Cancer Cells, Front. Oncol., 8 (2018) 376.
30. R.D. Sicchieri, W.A. da Silveira, L.R.M. Mandarano, T.M.G. de Oliveira, H.H.A. Carrara, V.F. Muglia, J.M. de Andrade, D.G. Tiezzi, ABCG2 is a potential marker of tumor-initiating cells in breast cancer, Tumor Biol., 36(12) (2015) 9233-9243.
31. J. Calahorra, E. Martinez-Lara, J.M. Granadino-Roldan, J.M. Marti, A. Canuelo, S. Blanco, F.J. Oliver, E. Siles, Crosstalk between hydroxytyrosol, a major olive oil phenol, and HIF-1 in MCF-7 breast cancer cells, Sci. Rep-Uk., 10(1) (2020) 6361.
32. B. Corominas-Faja, E. Cuyas, J. Lozano-Sanchez, S. Cufi, S. Verdura, S. Fernandez-Arroyo, I. Borras-Linares, B. Martin-Castillo, A.G. Martin, R. Lupu, A. Nonell-Canals, M. Sanchez-Martinez, V. Micol, J. Joven, A. Segura-Carretero, J.A. Menendez, Extra-virgin olive oil contains a metabolo-epigenetic inhibitor of cancer stem cells, Carcinogenesis, 39(4) (2018) 601-613.
33. O. Leis, A. Eguiara, E. Lopez-Arribillaga, M.J. Alberdi, S. Hernandez-Garcia, K. Elorriaga, A. Pandiella, R. Rezola, A.G. Martin, Sox2 expression in breast tumours and activation in breast cancer stem cells, Oncogene, 31(11) (2012) 1354-65.
34. S. Erdogan, O. Doganlar, Z.B. Doganlar, R. Serttas, K. Turkekul, I. Dibirdik, A. Bilir, The flavonoid apigenin reduces prostate cancer CD44(+) stem cell survival and migration through PI3K/Akt/NF-kappaB signaling, Life Sci., 162 (2016) 77-86.
35. C.Y. Tian, D. Huang, Y.L. Yu, J.H. Zhang, Q.X. Fang, C. Xie, ABCG1 as a potential oncogene in lung cancer, Exp. Ther. Med., 13(6) (2017) 3189-3194.